ISSN 1330-3651 (Print), ISSN 1848-6339 (Online) https://doi.org/10.17559/TV-20221113121639
Original scientific paper

Experimental, Software and Topological Optimization Study of Unpredictable Forces in Bolted Connections

Kürşat TANRIVER*, Mustafa AY

Abstract: Bolts cannot be loaded axially according to real field conditions in assembly lines. The main reasons for this are that the loads cannot be applied centred due to the plate thickness and the holes are wider than the bolt. This creates a change in the shear loads on the plate connections due to the moment. Therefore, in this study, a software including additional equations has been developed to reveal the moment formation which the bolts are exposed to. This program, prepared in Matlab software, first determines whether the material properties and thickness of the plate can withstand this tensile force when two bolt-connected plates are subjected to tensile force. If the plate is resistant to these tensile forces, the calculation is continued and the maximum shear stress on the bolts is calculated. For the experimental study, 5 samples with M6 bolt connections were prepared and tensile tests were carried out. The accuracy was measured by comparing the software result with the tensile tests and the finite element analysis results made in the Ansys program. In addition, a method for topology optimization is presented in order to improve the position of the connections on the plate.

Keywords: bolt; finite element; matlab; optimization; software

1 INTRODUCTION

When we examine the fasteners in general, there are many fastening methods, and some of them are used as the main method. Rivets were used first, then bolts and then welded joints [1].

Shear stress has a significant impact on the structural behaviour of bolted steel construction assemblies. There are studies using bolted plates to increase the bending capacity of beams [2]. It is known that bolts show significant differences in strength under combined load [3].

Qi et al. [4] created an optimization model on the tie plate on the train tracks. A finite element model of the angled guide plate is made, which is used to analyse the effects of bolt hole length, width, depth and number of holes on the force distribution along the plate.

Ribeiro dos Santos et al. [5] presented a study of the behaviour of bolts. Zhou et al. [6] experimentally investigated the buckling caused by bending by fixing the stainless-steel pipes with bolt connections through the plate. They also carried out a study that presented them numerically. Li and Genç [7] conducted an experimental study on open section members under eccentric load used in steel structures.

In order to examine the static behaviour of bolted connections, analysis methods that provide stress distribution can be developed and finite element models can be used to check their suitability [8].

For example, Weis et al. [9] conducted the necessary studies to investigate the effect and modal properties of bolted connections.

Rajanayagam et al. [10] investigated the load-deformation behaviour by testing with varying bolt sizes and hole tolerances. They then compared the results with the results of the Ansys finite element program.

Han et al. [11] simulated experimental materials with Abaqus software and compared the results. He et al. [12] investigated the high-temperature load distribution of a bolt joint structure. A two-dimensional asymmetrical model of the bolt connection structure was created and a modification of the standard metric thread profile was made according to the thread load distribution, taking into account certain properties. Maljaars and Euler [13] presented a study evaluating fatigue tests on bolted connections. Arjomandi et al. [14] tested five one-to-one scale specimens of bolted double-angle shear joints and monitored their load-deformation behaviour using digital image correlation technique. Elsabbagh et al. [15] investigated the joint rigidity of a steel profile bolted to the flange according to the bolt diameter, tightening moment, shear force, thickness of the bonded plates and the static/dynamic load parameters and verified with the finite element program. Zaroug et al. [16] connected the boards to each other with bolts only, adhesive only, and bolt and adhesive joint. They experimentally investigated the stiffness of the joint depending on the material type and thickness of the plates.

Rakotondrainibe et al. [17] performed a topology optimization study for potentially the shape of each part, the position and number of bolts, when considering bolted parts. Harl et al. [18] prepared a finite element model for the topology optimization of load-bearing structures. They also emphasized the importance of modelling the boundary conditions appropriately. Marzbanrad and Hoseinpour [19] performed a topology and shape optimization of a MacPherson control arm to obtain a lighter weight. Then, topology optimization was performed using HyperMesh software according to the fatigue life criterion.

Tensile test experiments can be done to investigate the tensile performance of the fastener [20]. In the literature, there are many studies in which the tensile load test results of bolts are made by both experimental and finite element methods and the results are compared [21]. In this study, in addition to these, calculations were made with software with an improved equation.

In this article, literature studies were examined and in addition to the studies here, calculations were made with a software. This software has an improved set of equations. This calculation consists of expressing the moment effect caused by the eccentric connection of the plates, as an equation. In order to reach the final goal of these equations, a code was written in Matlab program for the commonly used bolted connections. Thanks to this code, it can be determined whether the fastener withstands static forces or

not. In addition, the software results were compared with the finite element method and experimental results to measure the accuracy of the software. According to these results, a topology optimization model was studied for the verified program and added to the article.

2 MATERIAL AND METHOD

2.1 Material

For this study, 5 test samples of the same type and characteristics were prepared. The dimensions of the prepared test sample are shown in Fig. 1. For the sample, a 10 mm thick ST 37 plate and zinc-plated M6 steel bolts were used for the connections. For the sample, a 10 mm thick ST 37 plate and zinc-covered M6 steel bolts were used for the connections. The length of the bolts is 60 mm and has been selected as hexagon head, 8.8 quality and full thread according to DIN 933 standard.

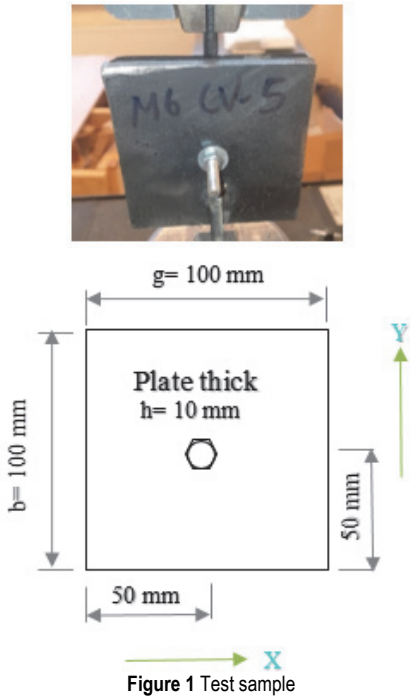

Figure 1 Test sample

2.2 Method

ISO 6892-1:2016 and ASTM E8:2016 standards are the leading standards used internationally in the tensile tests of metal materials [22]. The experimental setup for this study was prepared in accordance with the ISO 6892-1:2016 standard. Experiments were carried out on the Instron 5569 device. The test sample is formed by connecting two plates on top of each other with a single bolt right in the middle. Here, 5 specimens with the same properties were given a tensile load by the action of the upper jaw, with the lower jaw fixed, respectively, and the bolt was forced to be shorn between two plates. The load was gradually increased with a tensile speed of 2mm/min for each sample and the test was terminated when the bolts were shorn. The visual of the first test sample and the test device during the test is given in Fig. 2.

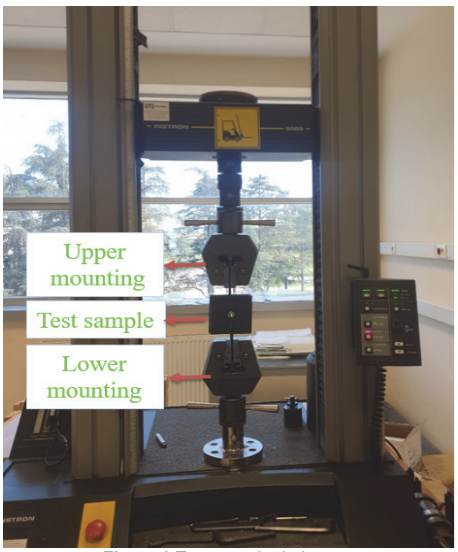

Figure 2 Test sample during test

As in many studies, the finite element analysis method was used in addition to the tensile test in this study [8, 9, 27]. Numerical analysis of experimental studies on buckling of shells can be done in Ansys program for finite elements [23]. In this study, finite element analysis was performed in the structural analysis module of the Ansys R19.2 program and then shear stresses were examined.

3 RESULTS AND DISCUSSION

3.1 Experimental Study and Finite Element Analysis

The experimental samples were given the names M6-Cv-1, M6-Cv-2, M6-Cv-3, M6-Cv-4, M6-Cv5, respectively. The tensile test was applied to the test samples one by one in the above-mentioned order. After the tensile test, the bolts broke after a certain stress. The final state of the test samples is shown in Fig. 3.

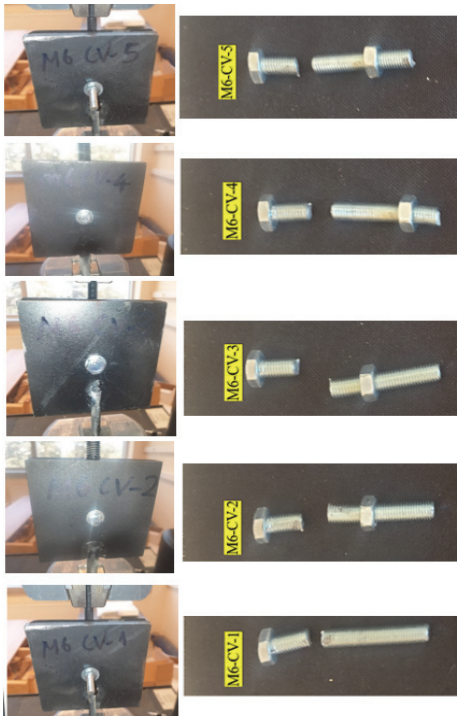

Figure 3 Final state of test samples

The stress-strain curves of the specimens as a result of the tensile tests are given in Fig. 4.

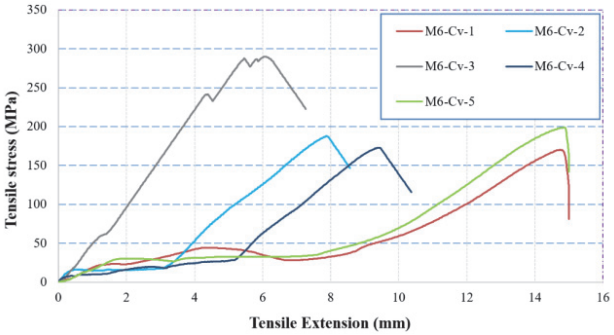

Figure 4 Stress-extension curves

Although the test specimens were geometrically identical to each other before the tensile test, they differed as a result of the test. For some, they showed much more extension than others, and rupture occurred at low tensile force. Some showed more noticeable bending. The stress-strain curves formed as a result of the tensile tests of the samples are given in Fig. 4, respectively. Values summary of the test results are given in Tab. 1.

Table 1 Tensile test result summary

Test specimens	Tensile extension / mm	Tensile stress / MPa	Load / Newton/N
M6-Cv-1	14.73	170.08	10204.56
M6-Cv-2	7.85	187.69	11261.14
M6-Cv-3	12.10	289.94	17379.37
M6-Cv-4	9.37	172.81	10368.61
M6-Cv-5	14.83	198.89	11933.46
M6-Cv-1	14.73	170.08	10204.56
M6-Cv-2	7.85	187.69	11261.14
Average value		203.88 MPa	12229.42

According to these results, when the arithmetic average of the tensile test stresses of 5 specimens with M6 Connection is taken, it is seen that the average stress is 203.88 MPa. Again, according to the same results, when the average shear loads of the bolts are taken, it was determined that the average shear load was 12229 N.

It is planned to carry out targeted studies by using the data obtained from the test results both in finite element analysis in Ansys R19.2 program and in matlab program. Therefore, in the Software section, it is aimed to write code based on the equations we developed for this study in the Matlab program.

In the Structural analysis module of the Ansys R19.2 program, the analysis was performed by applying a load of 12229 N, which is the average of the shear forces, to the same sample. A total of 235804 finite elements and 985717 nodes are used in the analysis. The mesh size was set to 1 mm using the sweep meshing method.

It was defined as surface-to-surface contact between plates. Again, the connection contact between plate-bolt groove and tooth was defined as surface-to-surface contact. In addition, tangential behaviour and normal behaviour for surface-to-surface contact, penalty friction and hard contact, respectively, were defined. To simulate the real constraints in the tests, fixed support in the y direction was defined to constrain the displacement of one of the two plates shown in Fig. 1. Problem was solved with Maximum Shear Stress. The stress field is shown in Fig. 5.

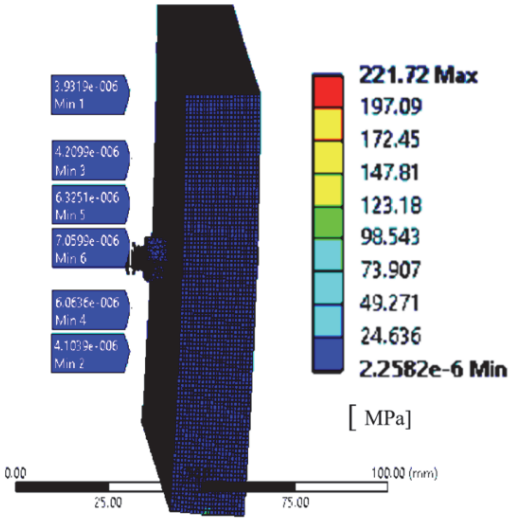

Figure 5 Finite element model Stress field

Accordingly, the maximum shear stress in the finite element analysis was 221.72 MPa. The ratio between the average of the test results in Tab. 1 and the finite element analysis result is 1.09.

Likewise, when we examine the studies in the literature, the ratio between the experimental results and the finite element analysis result is 1.77 in the study of Guo et al. [20], 1.08 in the study of Rajanyam et al. [10] and 1.02 in the study of Nguyen et al. [24]. The value in our study seems to be in-between the values in existing studies.

3.2 Modelling the Plate Under Moment and Software

The contact surface of the bolt holes providing the bolt-plate interaction should be taken into account [25]. The size and geometry of the bolt hole have a great influence on the joint resistance. It is known that in cases where the plate thickness is less than or equal to the thickness of the column wall, bending of the plate can lead to fracture [26].

It has been observed that there are studies investigating the effect of tightening torque and comparing them with analytical formulas, experimental work and simulations when the boards are connected only with bolt and bolt-adhesive connections [3, 8, 20]. However, no equational study of the moment effect caused by the eccentric connection of the plates has been found.

In order to calculate the torque value here, the centre of rotation of the connection must be found. It is not necessary to calculate the effects of the mentioned eccentric moment. For this, besides the basic equations and concepts, it is necessary to determine the number of bolts in this design and their coordinates on the plate.

In this working model, the equations developed to calculate the moments due to eccentricity are added. In the tensile test, the moments caused by the eccentricity in the connections of the plates were added to the program. A constant k was found between moments and distances by using parameters such as the centre of rotation, the coordinates of the rotation centres, the distance between the centres of rotation coordinates, the squares of the distance, the sum of the squares of the distance. An n expression to be defined to the system beforehand

determines the total number of bolts in the joining zone and at the same time n number of repetitions of operations to be performed. In the case study, an efficient numerical method behaviour has been studied, taking into account the effects of both bolt slip and bedding.

The section showing the plate, bolt, force and rotation centers is shown in Fig. 6.

The plate and its connections are shown in Fig. 6. Here, *h* is the plate thickness, *g* is the plate width, *d* is the diameter of the rod where the pulling jaws are attached, *m* is the effective length of the rod connection, *G* is the plate centre of gravity, and *F* is the direction of force applied by the pulling forces.

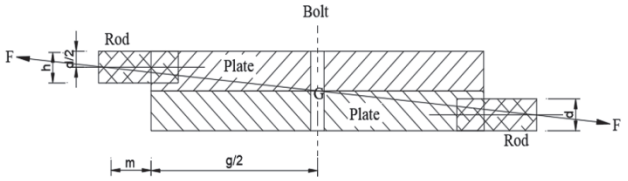

Figure 6 Test sample section Plane

Due to the angle below the tensile force direction, two forces, one horizontal and one vertical, will occur to the plates. The moments created by these two forces are in the same plane, but the directions of the moments are opposite to each other. The α angle that will occur in the section plane is shown in Fig. 7.

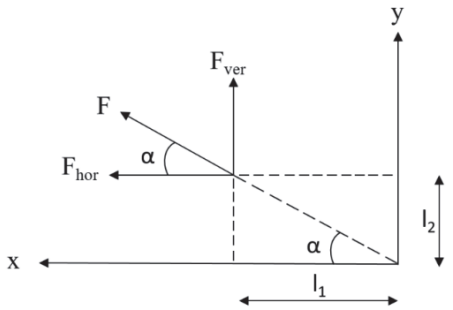

Figure 7 Angle in the section plane

Here, F_{vert} is the vertical force and F_{hor} is the horizontal force. Also, α, F_{vert} and F_{hor} are expressed in the equations below, where the distance of the vertical force from the center of rotation is l_1, the distance of the horizontal force from the center of rotation is l_2.

$$\alpha = \tan^{-1} l_2 / l_1 \tag{1}$$

$$l_2 = h - (d/2) \tag{2}$$

$$l_1 = (g/2) + m \tag{3}$$

$$F_{vert} = F \sin\alpha \tag{4}$$

$$F_{hor} = F \cos\alpha \tag{5}$$

The equations are given below: moment M_{vert} created by vertical force, moment created by horizontal force M_{hor}, net moment M_{net}, bolt shear stress τ_{bolt} and the resultant force F_{res}.

$$M_{vert} = F_{vert} l_1 \tag{6}$$

$$M_{hor} = F_{vert} l_1 \tag{7}$$

$$M_{net} = M_{vert} - M_{hor} \tag{8}$$

$$A_{bolt} = \pi D_{bolt}{}^2 / 4 \tag{9}$$

$$\tau_{bolt} = F_{res} / A_{bolt} \tag{10}$$

Here, D_{bolt} bolt diameter denotes A_{bolt} bolt cross-sectional area.

Plate thickness *h*, plate width *g*, moment of inertia in the moment direction I_z and tensile-compression stress $S_{t/c}$ due to M_{net} are given below.

$$S_{t/c} = M_{net} / Y_{max} / I_z \tag{11}$$

Considering the bending moment that will occur in the plates and the neutral axis depending on this bending moment, a tensile-compressive stress is created in the plate. As a result of this tensile-compression stress, an additional virtual shear force will occur in the plate that will act in the opposite direction to the bolts. It is seen that the sum of this virtual shear force and the shear forces acting on the plate during the tensile force will be equal to the shear force or active shear stress that actually breaks the bolts. For this virtual shear force, the surface area of the bolts must be found in the crush area, not the shear area.

Crush area A_{cr} with plate thickness h and virtual shear force F_{im} are shown by the following equation.

$$A_{cr} = hD_{bolt} \tag{12}$$

$$F_{im} = S_{t/c} A_{cr} \tag{13}$$

The F_{im} virtual force is the maximum amount of force that will act when the stress profile is considered to be triangular. Along with the remaining length of the bolt in the plates, its intensity also changes at that rate. Therefore, the average force corresponding to the area of this triangle will be half the F_{im} force. The lines of force are shown in Fig. 8.

The total shear force F_{sh} per bolt and the net shear stress τ_{net} per bolt are given in the following equations.

$$F_{sh} = F_{hor} + F_{im} / 2 \tag{14}$$

$$\tau_{net} = F_{sh} / D_{bolt} \tag{15}$$

Up to the point, a code has been written to calculate the bolt and plate strength of two bolted plates under load. Now, the software will be introduced and the software results will be compared with the results of both experiment and finite element analysis.

It is known that the eccentricity ratio in the load test can reduce the load carrying capacities.

The program has reached the final goal by adding some basic formulas to calculate the bolt strength and

additionally the moments suffered by the bolts in the experimental setups. When the two bolted plates are subjected to tensile force, the program first determines whether its material properties and thickness can withstand this tensile force. If the plate is resistant to these tensile forces, the calculation is continued and the maximum shear stress on the bolts is calculated.

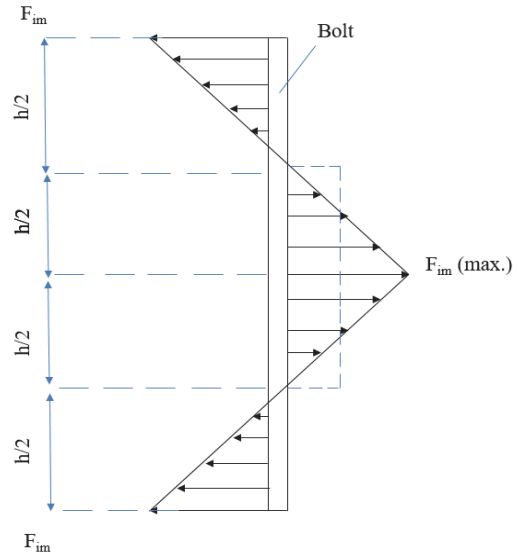

Figure 8 Force lines

When the arithmetic average of the tensile test results shown in Tab. 1 of 5 specimens with M6 Connection is taken, F_{real} load is 12229 N and τ_{real} stress is 203.88 MPa.

Accordingly, 12229 N F_{real} load was used in the finite element analysis and the stress result τ_{ans} was 221.72 MPa. Now, it is calculated in the matlab program with the equations we have developed. As a result of Matlab software, the critical stress increased to 220.70 MPa.

According to the results here, the results of my designed matlab software were 16.70 MPa higher than the τ real (203.88 MPa), which is the average of the M6 bolt-connected specimen test results made in the laboratory. In addition, it was found to be almost the same as the Ansys finite element analysis program result and less than 1.18 MPa. Matlab program flow procedure is given in Fig. 9.

The error rate of the Matlab program results was found according to both the experiment and the Anys finite element method results. The error rates are given below, with the error rate Err testRate according to the laboratory test results, and the error rate Err ansRate according to the Ansys finite element analysis results.

$$\text{Err testRate} = \left(\tau_{net} - \tau_{real}\right) / \tau_{real} \tag{16}$$

Here, τ_{net} = 220.70 MPa, τ_{real} = 203.88 MPa, the error rate Err testRate = 8.2 % was found.

$$\text{Err ansRate} = \left(\tau_{net} - \tau_{ans}\right) / \tau_{ans} \tag{17}$$

Here, τ_{net} = 220.70 MPa, τ_{ans} = 221.72MPa and error rate Err ansRate = −0.46 % was found.

In the literature research, there are studies indicating that the bolt geometry is improved when compared with the existing models and that the moment is created when the loads are connected eccentrically [2, 3, 8, 20]. However, no study has been found that develops and explains them with additional formulas by putting them into equations.

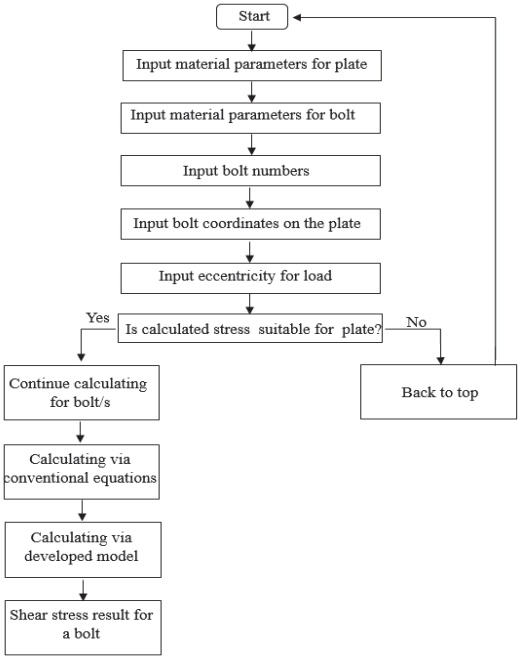

Figure 9 Flowchart of the software procedure

3.3 Topology Optimization

Optimization is a method of optimizing a system, usually using mathematical operations to achieve the best possible result. Determination of basic configurations, definition of design variables, definition of objective function, selection and application of appropriate optimization problems are defined as optimization steps.

Using the optimization steps mentioned in this article, a study has been made for the topology where the bolted plates will be subjected to minimum load according to the given data. Users are expected to give the number of bolts, the distance of the bolts to the plate edges, the distances of the bolts to each other, the desired safety factor for the plate material and the desired safety factors for the bolt connections. According to these data, in this optimization study, it is aimed that the bolts carry the optimum load in the optimum arrangement as much as possible. Here, it is undesirable for some of the bolts to carry a maximum load by carrying less and some more load. One of the goals here is to ensure that all bolts are subjected to loads as close to each other as possible, even if they are not equal to each other at the desired factor of safety. Thus, the security of the structure in which these connections will be used is ensured by subjecting the bolts to loads close to each other.

Optimization can be used for train tracks [4], shape of bolt [17], load-bearing structure [18], Control arm [19], air tanks [27], bolt strength [28], cutting parameters [29], machine learning [30].

Purpose and constraint functions should be created in accordance with the classical optimization study. In this

study, it is aimed to position the bolt connections in the best way.

- Minimum stress should occur in sheet tearing.
- Minimum stress should occur in bolt tension and safety factor should be maximum.
- The torsional, bending and buckling values of the plates must remain below the determined values.

In line with these goals, a target function study has been carried out to ensure that the connections are placed in the most appropriate way.

The schematic drawing prepared to define the constraint function and the critical stress zone is shown in Fig. 10.

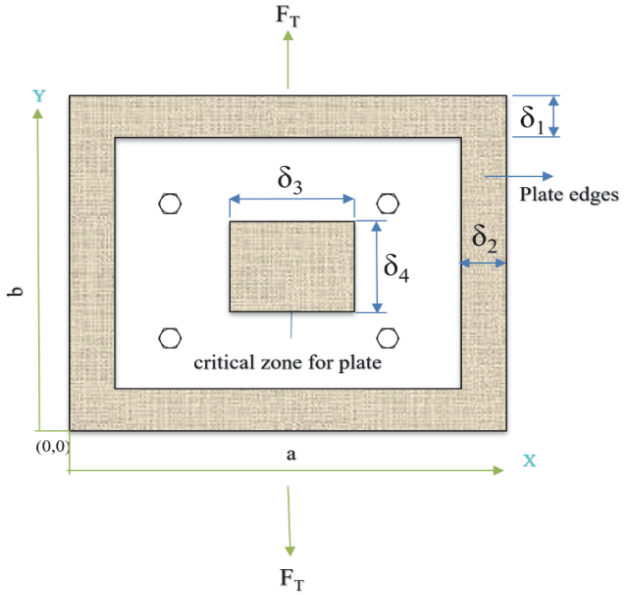

Figure 10 Critical stress zones

In terms of plate tearing, the bolts are not placed at certain distances δ_1 and δ_2 of the plates. Otherwise, the plate would remain in the unsafe area for tearing.

The area between the inequalities is A_1, the critical zone is A_2, and the related equations are given below.

$$\delta_2 \le x \le a - \delta_2 \tag{18}$$

$$\delta_1 \le y \le b - \delta_1 \tag{19}$$

$$A_1 = xy;\ A_2 = \delta_3\delta_4 \tag{20}$$

The bolts are located at a certain distance L_1 relative to each other. This distance shown in Fig. 11 represents the minimum distance between the connections.

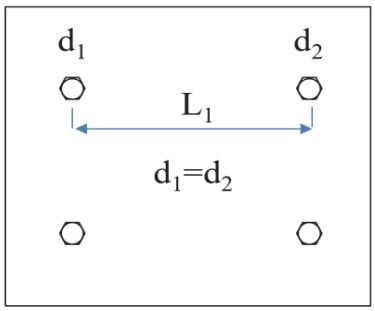

Figure 11 L_1 distance

This L_1 distance is determined by empirical laws and in reality, they should be at least 2 bolt diameters apart. If a value closer to these values occurs, ruptures may occur at sudden and low stresses, since a dangerous and plastic zone will be formed due to the residual stress that occurs during manufacturing. The L_1 distance value is expressed below.

$$L_2 = 2d_1 = 2d_2 \tag{21}$$

In terms of torsion and bending values, rotation and collapse values must be below a certain value. The torsion and bending equations are given below, where G and E are constants due to materials, I_{bc} and I_b are torsion and bending moments of inertia.

$$\text{Buckling rigidity} = GI_{bc} \tag{22}$$

$$\text{Bending rigidity} = EI_b \tag{23}$$

In order for the torsional and bending moments to be below a certain value, the moments of inertia I_{bc} and I_b must be at their maximum value. For this, the bolt connections should be as far apart as possible.

However, torsional, bending rigidity and stresses must yield consistent results under loads acting on the plate. In order to achieve this, the collapse and rotation values should be close to each other in every part of the plate, and the safety coefficients of the fasteners should be as close to each other as possible due to the homogeneous distribution of the fasteners and the loads on them. In other words, the factor of safety S must be in a certain range. It is expressed below.

$$S = [S_{max}, S_{min}] \tag{24}$$

If the target function is formulated with S being the factor of safety the factor of safety should be maximum and the factor of safety of each fastener should be close to each other. The factor of safety is given below, with the allowable shear stress τ_{alw}.

$$S = [\tau_{alw} / \tau_{max}] \tag{25}$$

The forces acting on the fasteners are shown in Fig. 12. Plate centre of gravity G, tensile force per fastener F_n, angle between forces acting on fasteners due to moment and forces acting due to tensile load α, bolt cross-sectional area, perpendicular force F_m opposing the moment trying to rotate the plate in fasteners, the resultant force associated with them F_{res} are expressed below.

$$F_{res} = \sqrt{F_n^2 + F_m^2 + 2F_n F_m \cos\alpha} \tag{26}$$

To resist the moment, k and F_m are expressed as follows, with k being a constant in the input part of the software.

$$k = \frac{F_{m1}}{r_1} = \frac{F_{m2}}{r_2} = , ..., = \frac{F_{mn}}{r_n} \tag{27}$$

$$F_m = k \cdot r_n \tag{28}$$

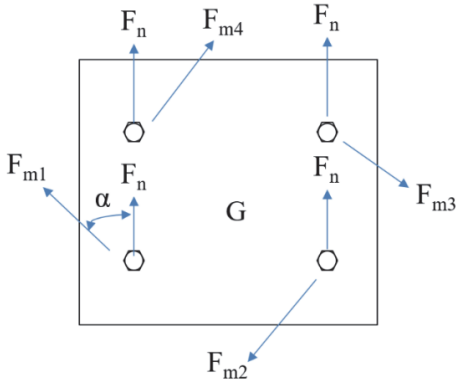

Figure 12 Force on bolts

These are expressed by the following equations: the distance r between the centres of rotation coordinates, the distance squared R, and the sum of the distance squares R_S, the moment and k, a constant between the distances.

$$R = r^2 \tag{29}$$

$$R_s = \text{sum}(R) \tag{30}$$

$$k = M_z / R_s \tag{31}$$

Expressed as a constant number, k decreases as R_S increases. Therefore, it seems that it is possible to reduce the moment-induced F_m forces by increasing the moment arm distance R_S.

A force F_n is considered constant because it depends on the number of fasteners. F_m forces, on the other hand, can be assumed to be directly proportional to r_n. The variable part in the F_{res} resultant force expressed in Eq. (26) above is given below.

$$\text{variable in equation} = 2F_n F_m \cos\alpha \tag{32}$$

The resultant force F_{res}, with constant forces F_{cons}, variable forces F_{var}, is shown below in a different expression.

$$\overrightarrow{F_{res}} = \overrightarrow{F_{cons}} + \overrightarrow{F_{var}} \tag{33}$$

The number of rows is i, the constant S_{cons}, the variable S_{var}, and the safety factor S_{sum} is expressed as a total below.

$$S_{sum_{(i)}} = S_{cons_{(i)}} + S_{var_{(i)}} \tag{34}$$

The graph between the change in the factor of safety and the number of fasteners i is shown in Fig. 13.

Our aim here is to reduce the S_{max} and S_{min} intervals in fasteners as much as possible and to achieve an equal value as much as possible, although not an equal S number for all bolts. In fact, an equal value must be achieved, all connections must be in the same coordinates.

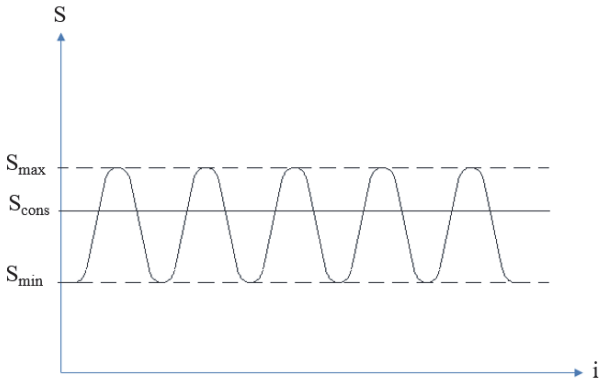

Figure 13 Safety factor scatter chart

In other words, for the direction and intensity of the moment-induced force to be the same, all connections must overlap. This will not be possible under real conditions. However, even though the direction is not the same, it is possible with a circular arrangement system to have the same F_m force in the fasteners. It ensures that the F_m force aligned at a certain radius and at a certain angle is the same, which is beneficial to stabilize the factor of safety at a certain level. The bolt-rivet arrangement is shown in Fig. 14, where the Tensile Force F_T is the distance e between the pulling force and the centre of gravity.

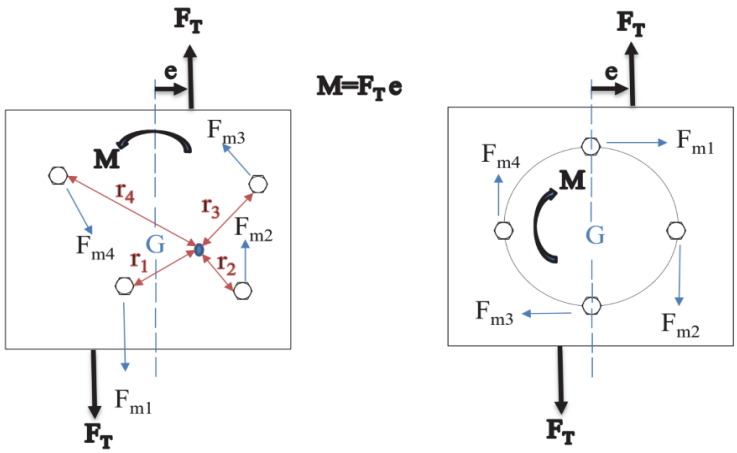

Figure 14 Bolt arrangement on plate: (a) Random (b) Circular

It is stated that all F_m force intensities are the same when a circular arrangement is made on the plate. Therefore, considering the varying function in Eq. (32), the cosα value will vary here due to the direction of the F_m forces. After the variability here is fully analysed, it will be revealed which parameters our resultant force F_{res} target function will consist of. The said α value is an angle between F_m and F_n.

The relation between F_m and F_n, where A is a constant number, is expressed below.

$$F_m = AF_n \cos\alpha \tag{35}$$

If we substitute this expression in Eq. (32), the resultant force F_{res} is expressed below.

$$F_{res} = \sqrt{F_n^2 + F_m^2 + \text{number} \cdot F_m^2} \tag{36}$$

It is already known that F_n is a constant in this equation.

The expression can be written as follows.

$$F_{res} \cong \sqrt{F_m^2 + \text{number} \cdot F_m^2} \tag{37}$$

$$F_{res} \cong \sqrt{\text{number} \cdot F_m^2} \tag{38}$$

Here, if the constant S_a is called in the number value, the resultant force F_{res} can be written as follows. Here it turns out that the resultant force F_{res} value is directly proportional to r_n.

$$F_{res} = S_a F_m \tag{39}$$

$$F_{res} = S_a k r_n \tag{40}$$

We can summarize this section as follows.

It has been revealed that this function, with our objective function S, is directly related to the resultant force F_{res}. Since the resultant force F_{res} is directly proportional to the distance r_n, it is necessary to keep all bolt-rivet S values close to each other in order to stabilize the safety factor as much as possible. For this, it is necessary to increase the r_n value, which is the bolt-rivet moment distances, as much as possible. This is possible by making the bolt arrangement circular and especially at the maximum radius.

4 CONCLUSION

There are studies in which the bolt geometry has been improved compared to the existing models. Tensile tests are performed to investigate the tensile performance of the fastener. Generally, there are studies in which experimental results and finite element analysis results are compared. There are also studies confirming the numerical and experimental results for estimating the shear capacity of bolted connections.

In addition, in this study, calculations were made with the help of Matlab software and the results were compared with the results of both finite element and experimental methods in the form of triple verification method. In addition to conventional studies, the Matlab software has been improved by adding codes to calculate the moments of eccentricity during tension. In addition, a method has been developed for Topology optimization in order to improve the position of the connections on the plate. In addition, a method has been developed for Topology optimization in order to improve the position of the connections on the plate. With this method, it is ensured that all bolts are subjected to loads as close to each other as possible, even if they are not equal to each other in the desired safety factor. Thus, the security of the structure in which these fasteners will be used can be ensured by subjecting the bolts to loads close to each other.

Although the test samples were geometrically identical to each other before the tensile test, they showed differences in the test result. For some, by showing much more elongation than for others, some rupture occurred at low tensile force. Some showed more noticeable bending. According to the test results, when the arithmetic average of the tensile test stresses of 5 identical specimens with M6 Connection is taken, it is seen that the average stress is 203.88 MPa. Again, according to the same results, when the average shear loads of the bolts were taken, it was determined that the average shear load was 12229 N.

Finite elements with an average shear load of 12229 N as a result of the experiment were made in the Structural analysis module of Ansys R19.2 program. Accordingly, the maximum shear stress in the finite element analysis was 221.72 MPa. Considering these values, the ratio between the average of the results and the finite element analysis result is 1.09. It is seen that this result is a value between the experimental results in the literature and the ratios of the finite element analysis results. It is seen that this result is a value between the experimental results and the ratios of the finite element analysis results in the literature.

In addition, the code written with additional equations was run in the Matlab program with an average shear load of 12229 N as a result of the experiment and the critical stress was 220.70 MPa. Matlab program results showed that M6 bolted specimens were 16.70 MPa higher than the tensile test stress result average. Also, it was found to be almost the same as the Ansys finite element analysis program result and less than 1.18 MPa. Matlab software results written with improved additional formulas. It is seen that the error rates are 8.2% based on the experimental results, and −0.46% based on the Ansys finite element analysis program results.

In addition, the topology optimization results can be summarized as follows:

- Although our objective function appears to be radical expression and trigonometric, it has been found that it is equivalent to a linear equation in the calculations.
- It has been seen that a clock arrangement as wide as possible in the bolt arrangement will minimize the resulting stresses and stabilize the variables.
- It is known that it is necessary to increase the moment of inertia of the plates in order to increase the bending-torsional rigidity. This is possible by increasing the distance between the bolts. Thus, it turns out that the region that resists rotation and bending is actually the space between the fasteners.

In the future, it is planned to develop the software of the linear topological optimization program, where the regions that the fasteners cannot enter are determined, and where we can adjust the maximum safety factor and stiffness in the clock sequence depending on the radius.

5 REFERENCES

[1] Albiez, M., Damm, J., Ummenhofer, T., Kaufmann, M., Vall'ee, T., & Myslicki, S. (2022). Hybrid joining of jacket structures for off Shore wind turbines. Determination of requirements and adhesive characterisation. *Engineering Structures*, *259*(2), 114-186. https://doi.org/10.1016/j.engstruct.2022.114186

[2] Yao, Y., Huang, H., Zhang, W., Ye, Y., Xin, L., & Liu, Y. (2022). Seismic performance of steel-PEC spliced frame beam. *Journal of Constructional Steel Research*, *197*(107456), 1-11. https://doi.org/10.1016/j.jcsr.2022.107456

[3] Pitrakkos, T., Tizani, W., Cabrera, M., & Salh, N. F. (2021). Blind bolts with headed anchors under combined tension and shear. *Journal of Constructional Steel Research*, *179*(107456), 1-12. https://doi.org/10.1016/j.jcsr.2021.106546

[4] Qi, W., Aela, P., Jing, G., Tong, Y., & Movahedi Rad, M. (2022). Optimization of the Angled Guide Plate for the Vossloh W14-PK Fastener. *Acta Polytechnica Hungarica*, *19*(6), 163-182. https://doi.org/10.12700/APH.19.6.2022.6.12

[5] Ribeiro dos Santos, L., Barreto Caldas, R., Prates, J. A., Rodrigues, F. C., & Cardoso, H. d. S. (2022). Design procedure to bearing concrete failure in composite cold-formed steel. *Engineering Structures*, *256*(1), 114003. https://doi.org/10.1016/j.engstruct.2022.114003

[6] Zhou, F., Huang, L., & Li, H. T. (2022). Cold-formed stainless steel SHS and RHS columns subjected to local-flexural interactive buckling. *Journal of Constructional Steel Research*, *188*(106999), 1-12. https://doi.org/10.1016/j.jcsr.2021.106999

[7] Li, Q. Y. & Genç, B. (2021). Tests of cold-formed steel built-up open section members under eccentric compressive load. *Journal of Constructional Steel Research*, *84*(106775), 1-12. https://doi.org/10.1016/j.jcsr.2021.106775

[8] Hammamı, C. (2022). Nmerical investigation of static behavior of bolted joints. *Journal of Theoretical and Applied Mechanics*, *60*(3), 385-394. https://doi.org/10.15632/jtam-pl/150487

[9] Weis, P., Šteininger, J., Sapieta, M., & Patin, B. (2021). Modal Properties of Bolted Housing depending on the Methodology of a Solution of Bolted Joints. *Tehnicki Vjesnik, Technical Gazette*, *28*(5), 1711-1716. https://doi.org/10.17559/TV-20200131154541

[10] Rajanayagam, H., Gunawardena, T., Mendis, P., Pologanathan, K., Gatheeshgar, P., Dissanayake, M., & M. Corradi. (2022). Evaluation of inter-modular connection behaviour under lateral loads: An experimental and numerical study. *Journal of Constructional Steel Research*, *194*(107335), 1-16. https://doi.org/10.1016/j.jcsr.2022.107335

[11] Han, Q., Chen, S., Zou, J., Zhang, H., Liu, M., Ju, J., & Sang, X. (2021). Numerical study on the dynamic response of a concrete fillet steel tubular long column under axial impact by a rigit body. *Journal of Theoretical and Applied Mechanics*, *59*(141308), 551-563. https://doi.org/10.15632/jtam-pl/141308

[12] He, L., Zhang, B., Guo, C., & Shi, W. (2021). Stress and load distribution analysis in bolt connection with modified thread profile under high temperature conditions. *Journal of Theoretical and Applied Mechanics*, *59*(40220), 469-480. https://doi.org/10.15632/jtam-pl/140220

[13] Maljaars, J. & Euler, M. (2021). Fatigue S-N curves of bolts and bolted connections for application in civil. *International Journal of Fatigue*, *151*(106355), 1-15. https://doi.org/10.1016/j.ijfatigue.2021.106355

[14] Arjomandi, K., Matthews, J., & Wyman, B. (2021). Flexibility requirement of bolted double-angle shear connections. *Journal of Constructional Steel Research*, *184*(1), 1-9. https://doi.org/10.1016/j.jcsr.2021.106780

[15] El Sabbagh, A., Sharaf, T., Nagy, S., & ElGhandour, M. (2019). Behavior of extended end-plate bolted connections subjected to monotonic. *Engineering Structures*, *190*(1) 142-159. https://doi.org/10.1016/j.engstruct.2019.04.016

[16] Zaroug, M. E., Kadioglu, F., Demiral, M., & Saada, D. (2018). Experimental and numerical investigation into strength of bolted, bonded and hybrid single lap joints: Effects of adherend material type and thickness. International Journal of Adhesion and Adhesives, *87*(2018), 130-141. https://doi.org/10.1016/j.ijadhadh.2018.10.006

[17] Rakotondrainibe, L., Desai, J., Orval, P., & Allaire, G. (2022). Coupled topology optimization of structure and connections for bolted. *European Journal of Mechanics, A Solids*, *93*(1). https://doi.org/10.1016/j.euromechsol.2021.104499

[18] Harl, B., Predan, J., Gubeljaki, N., & Kegl, M. (2020). Influence of Variable Support Conditions on Topology Optimization of Load-Carrying Parts. *Tehnički vjesnik, Technical Gazette*, *27*(5), 1501-1508. https://doi.org/10.17559/TV-20191001212144

[19] Marzbanrad, J. & Hoseinpour, A. (2017). Structural Optimization of MacPherson Control Arm Fatigue Loading. *Tehnički vjesnik, Technical Gazette*, *24*(3), 917-924. https://doi.org/10.17559/TV-20150225090554

[20] Guo, X., Zong, S., Gao, S., Zhu, S., & Zhang, Y. (2020). Ductile failure of occlusive high strength bolt connections. *Journal of Constructional Steel Research*, *168*(105982), 1-15. https://doi.org/10.1016/j.jcsr.2020.105982

[21] Liu, Y., Li, M., Lu, X., Li, Q., & Zhu, X. (2021). Pull-out performance and optimization of a novel Interference-fit rivet for. *Composite Structures*, *269*(114041). https://doi.org/10.1016/j.compstruct.2021.114041

[22] İncesu, A., Ercan, B., Çevik, E., & Akgül, Y. (2022). Reference material development process for tensile test method. *Pamukkale University Journal of Engineering Sciences*, *28*(1), 58-62. https://doi.org/10.5505/pajes.2021.01613

[23] Karasev, A., Varianychko, M., Bessmertnyi, Y., Krasovsky, V., & Karasev, G. (2020). Numerical analysis of experimental research pn buckling of closed shallow conical shells under external pressure. *Journal of Theoretical and Applied Mechanics*, *58*(115321), 117-126. https://doi.org/10.15632/jtam-pl/115321

[24] Nguyen, T. T., Thai, H. T., Li, D., Wang, J., Uy, B., & Ngo, T. (2022). Behaviour and design of eccentrically loaded CFST columns with high. *Journal of Constructional Steel Research*, *188*(107004), 1-16. https://doi.org/10.1016/j.jcsr.2021.107004

[25] Ye, J., Quan, G., Yun, X., Guo, X., & Chen, J. (2022). An improved and robust finite element model for simulation of thin-walled. *Engineering Structures*, *250*(9), 1-25. https://doi.org/10.1016/j.engstruct.2021.113368

[26] Javora, A. & Skejić, D. (2017).Resistance Assesment of Beam-to- Column Joints with Different Blind. *Tehnički vjesnik, Technical Gazette*, *24*(4), 1103-1112. https://doi.org/10.17559/TV-20150923165859

[27] Petrik, M., Erdős, A., Jármai, K., & Szepesi, G. (2021). Optimum Design of an Air Tank for Fatigue and Fire Load. *Acta Polytechnica Hungarica*, *18*(3), 163-177. https://doi.org/10.12700/APH.18.3.2021.3.9

[28] Tanriver, K. & Ay, M. (2020). Topology Optimization of a Steel Construction Bolt Under Boundary Conditions. *Euroasia Journal of Mathematics, Engineering, Natural & Medical Sciences*, *7*(12), 31-47. https://doi.org/10.38065/euroasiaorg.272

[29] Basmaci, G., Kurt, M., Ay, M., & Bakir, B. (2018).

Optimization of the Effects of Machining Parameters in Turning on Hastelloy C22 Composition through Taguchi Response Surface Methodology. *Acta Physica Polonica Series a*, *134*(1), 28-31. https://doi.org/10.12693/APhysPolA.134.28

[30] Sun, Y. & Lin, C. M. (2021). Design of Multidimensional Classifiers using Fuzzy Brain Emotional Learning Model and Particle Swarm Optimization Algorithm. *Acta Polytechnica Hungarica*, *18*(4), 25-45. https://doi.org/10.12700/APH.18.4.2021.4.2

Contact information:

Kürşat TANRIVER, PhD
(Corresponding author)
Institute of Pure and Applied Sciences,
Mechanical Engineering Department,
Marmara University,
Göztepe, 34722 Istanbul, Turkey
E-mail: k.tanriver@hotmail.com

Mustafa AY, Professor
Faculty of Technology,
Mechanical Engineering Department,
Marmara University,
Maltepe, 34854 Istanbul, Turkey
E-mail: muay@marmara.edu.tr